

From the RSNA Refresher Courses

Cardiac MR Imaging: A Guide for the Beginner¹

Lawrence M. Bost, MD

The complex motion of the heart during contraction is a serious challenge to the diagnostic radiologist and to the capabilities of the magnetic resonance (MR) imaging unit itself, but electrocardiographic (ECG) gating “stops” motion and thus allows acquisition of diagnostic-quality images. Attention to placement of chest-wall ECG electrodes and the course of ECG leads from the patient will maximize the quality of the gating signal and result in better-quality images. Before commencing the MR imaging examination, the clinical questions for the examination must be identified so that a clinical protocol can be applied to acquire relevant morphologic and physiologic data. In addition to the standard orthogonal views (axial, coronal, and sagittal), oblique and complex sections parallel and orthogonal to intrinsic cardiac axes may be necessary to portray the relevant anatomy to best advantage. Construction of these views requires an understanding of basic normal and pathologic cardiac anatomy. If care is taken in the planning and execution of the MR imaging examination, the radiologist will be able to exploit this exciting technology to its full noninvasive potential.

Abbreviation: ECG = electrocardiography

Index terms: Aorta, dissection, 56.74, 94.74 • Heart, diseases, 50.14 • Heart, MR, 50.12141 • Heart, ventricles, 52.12141 • Pericardium, 55.12141

RadioGraphics 1999; 19:1009-1025

¹From the Department of Radiology, Beth Israel Medical Center, First Ave and 16th St, New York, NY 10003. Presented as a refresher course at the 1998 RSNA scientific assembly. Received July 28, 1998; revision requested August 26 and received September 25; accepted September 25. **Address reprint requests** to the author.

©RSNA, 1999

■ INTRODUCTION

Electrocardiographically (ECG) gated cardiac magnetic resonance (MR) imaging is useful for evaluating both congenital and acquired heart disease (1,2). Despite the usefulness of this technique, it remains underused in part due to the difficulty of managing heart disease; patients may be clinically unstable and often receive a constant infusion of cardioactive drugs. Furthermore, MR imaging suites are often recent additions to medical centers and have been sited in secluded areas away from the clinical core of the facility, a location that makes movement of patients to and from the imager difficult. Dependence on ECG gating for cardiac evaluation prolongs cardiac examination. Variation in intracardiac anatomy may be confusing and thus further prolong examination time by requiring additional views. We have found that many patients with heart disease, especially those with ischemic or cyanotic heart disease, are claustrophobic and may require additional anxiolytic or sedative medication before or during the examination.

In this article, ECG-gated cardiac MR imaging is reviewed. Specific topics discussed are acquisition techniques and pitfalls, planning the examination, performing the examination, indications for cardiac MR imaging, and completing the examination.

■ ACQUISITION TECHNIQUES AND PITFALLS

Cardiac MR imaging makes use of ECG gating to suppress motion artifacts caused by complex cardiac motion and great artery pulsation (3-5). In conventional MR imaging, the preset repetition time determines the timing of phase-encoding gradient stepping. Each phase-encoding step follows the previous step until an image of n phase-encoding steps (usually 256-512) is obtained. The length of time needed to obtain an image with one signal acquired is the number of phase-encoding steps times the repetition time. This scheme works well if the object being imaged does not move. One can imagine the image of a rapidly beating heart obtained with a continuous 15-second exposure time.

To suppress the periodic motion of cardiac contraction, ECG gating is used to provide a periodic timing function to image acquisition. In other words, rather than a series of phase-encoding steps being performed, each independent of a particular phase of cardiac contraction, the ECG R wave is used to signal the advancement of phase encoding. Each of the phase-encoding steps of an image is thus col-

lected from each of a series of heartbeats with each step obtained at the same phase (time delay after a reference point in the ECG cycle) of cardiac contraction. Phase-encoding step 1 is obtained from beat 1, phase-encoding step 2 is obtained from beat 2, and so on until data from all 256 or 512 phase-encoding steps are collected. The ECG gate thus tells the imager when to advance phase encoding. Therefore, an image made of 256 "strips" of the heart with each strip obtained at the same phase of the cardiac cycle will be a coherent image of the beating heart at that particular phase of the cardiac cycle and will be free of motion-related artifacts.

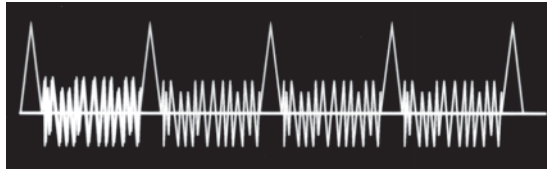
If the image is obtained at or very close to the R wave, then image acquisition correlates with electromechanical end diastole and an end-diastolic image is obtained. If the imager was instructed to wait two-thirds of the time between two R waves to step phase encoding, then a late systolic image would be obtained. The R wave is conventionally chosen as the gating signal because it has the greatest voltage and is therefore more easily identified from the ECG signal by the imager (Fig 1). If the voltage of the QRS complex is diminished (as in patients with pericardial effusion) or if the P- or T-wave voltage is increased (as in patients with atrial enlargement or hyperkalemia), then the imager may be "confused" and trigger off of a non-R wave; the result will be impaired image quality. That is, if the device senses an R wave followed by a P or T wave followed by another R wave and so on, the imager may presume a series of long followed by short followed by long R-R intervals and produce incoherent images (Fig 2).

Spin-echo acquisitions produce series of images with each series obtained at a different anatomic level within the chest and each image obtained at a different phase of the cardiac cycle. With this technique, several sections can be obtained in the same time that used to be necessary to obtain a single section. This technique has made cardiac MR imaging clinically feasible. However, since each image in such an acquisition is obtained at a different phase of the cardiac cycle, functional comparison of anatomic sections may be confusing if not impossible.

Short flip angle gradient reversal (gradient-echo) cine imaging (6,7) provides images with increased temporal resolution, which allows evaluation of ventricular function, valvular regurgitation or stenosis, and shunts. With this pulse sequence, the same anatomic section is excited with radio-frequency pulses by using a short repetition time. The temporal resolution of the examination depends on the repetition time and heart rate. In other words, a faster



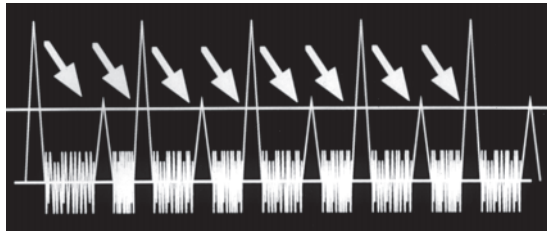
1a.



1b.



1c.



2.

Figures 1, 2. (1) ECG gating. (a) From an engineering point of view, the R waves should be precisely spaced and unambiguously greater in voltage than any other ECG signal. (b) In the clinical setting, differentiation of R waves from background noise may be less precise. (c) R waves are identified by comparing the voltage of a signal with a known ("threshold") voltage. Thus, an R-wave triggering signal is a signal greater than the threshold. Thus, an R-wave triggering signal is a signal greater than the threshold. (2) Pseudo-R-R intervals. If the T-wave voltage exceeds the threshold voltage, then the T waves are interpreted by the imager as R waves. The assumed R-R intervals (arrows) are unequal; the result is temporally irregular phase-encoding steps and subsequently incoherent images.

heart rate results in a shorter R-R interval (the time between R waves) and, for any given number of discrete phases of the cardiac cycle, less time between phases. After a fixed number of signals are acquired, the imaging system waits for the next R wave to advance to the next phase-encoding step.

Occasionally, an adequate ECG tracing may not be obtained. This problem may occur in patients with severe ventricular ectopia (eg, after

acute myocardial infarction) or arrhythmogenic right ventricular dysplasia or in patients with very low voltage ECGs (eg, patients with pericardial effusion). In these individuals, peripheral pulse gating may be used.

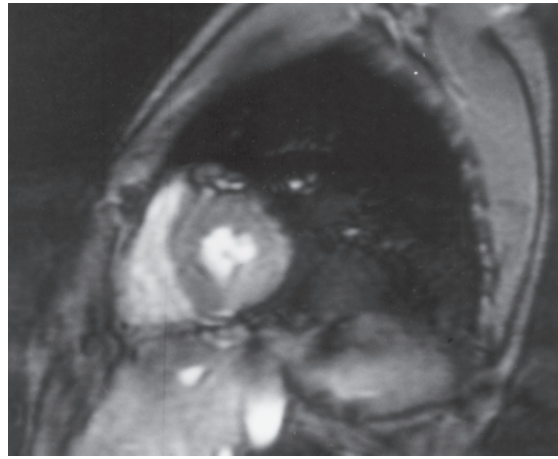
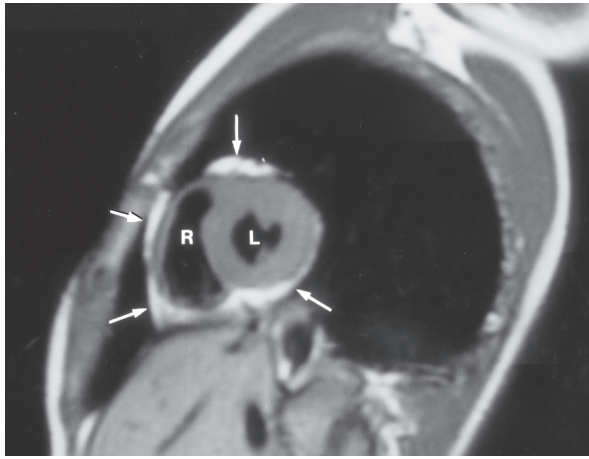
■ PLANNING THE EXAMINATION

Communication between the referring physician and the radiologist performing the examination is essential for efficient and accurate cardiac MR imaging. The purpose of the examination must be clear: to identify a specific problem or to confirm or exclude a specific diagnosis. For example, ruling out aortic dissection is a straightforward clinical problem. The MR imaging examination will naturally include evaluation of the pericardial space, the aortic valve and left ventricle, and the origins of the arch vessels. On the other hand, a referral for evaluation of "heart failure" is vague and makes performance of a complete examination difficult to achieve.

● Selecting a Pulse Sequence

For both spin-echo and gradient reversal pulse sequences, the spatial resolution of an MR image is dependent inversely on the size of the field of view and directly on the number of phase-encoding steps chosen. If morphologic analysis will provide the specific answer to a clinical question, then spin-echo acquisition, which provides the highest contrast resolution, should be used. The downside of spin-echo acquisition is the temporal resolution of the examination. The necessity to rephase spins by means of a second radio-frequency pulse (the 180° pulse) limits the number of images that can be obtained from a patient with a given heart rate. Thus, functional abnormalities may not be examined directly. Analysis of resultant morphologic changes (eg, diagnosing aortic regurgitation by demonstration of a dilated and hypertrophied left ventricle and dilated aorta) must suffice.

Cine imaging (gradient reversal images viewed in the loop cine mode) can be performed much more rapidly than performing series of 90° and 180° radio-frequency pulse pairs and therefore allows acquisition with greater temporal resolution, which is ideal for functional analysis (eg, diagnosis and quantitation of aortic regurgitation by direct demonstration of the signal void of the regurgitant jet). On the other hand, cine acquisitions have lower contrast resolution due to the short flip angle and short repetition time



a.

b.

Figure 3. Comparison of spin-echo acquisition with gradient reversal acquisition. (a) Midsystolic spin-echo MR image (short-axis section obtained 138 msec after the R wave) shows a difference in signal intensity between the left (*L*) and right (*R*) ventricular myocardium and the epicardial fat (arrows). (b) Gradient reversal MR image obtained in the same location at the same phase of the cardiac cycle shows that the difference in signal intensity between the cavity blood and the ventricular myocardium and between the myocardium and fat is markedly decreased.

used (Fig 3). Furthermore, they are more sensitive to artifacts caused by sternal sutures, valvular prostheses, or surgical clips. Although there is no improvement in contrast resolution, k-space segmented gradient reversal acquisitions are very rapid and may be used to overcome the acquisition time limitations of conventional gradient reversal sequences.

● Contraindications to Cardiac MR Imaging

Cardiac MR imaging is absolutely contraindicated in patients with an active pacemaker (8) or other implanted electrical stimulator, free particulate iron in the optic globe, or intracerebral aneurysm clips. Mediastinal sutures and clips do not contraindicate MR imaging. With the exception of pre-6000 series Starr-Edwards valves, there are no cardiac prostheses that pose a known risk to the patient or are adversely affected by examination at the magnetic field strengths presently used (<2 T). Untoward effects of MR imaging on cardiac support hardware, such as implantable ventricular assistance devices, are not well established. Thus, it is prudent to exclude patients with these devices from MR im-

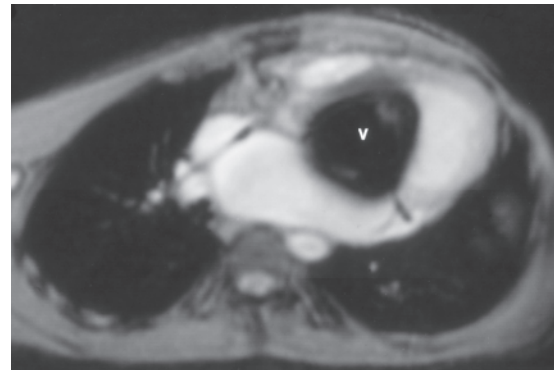
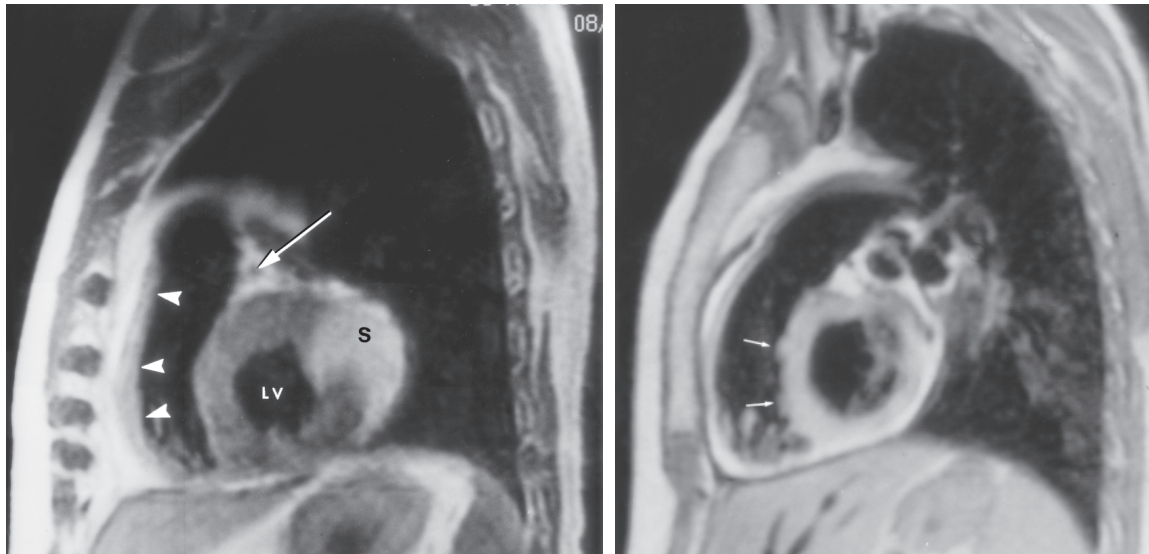


Figure 4. Image defect caused by an aortic valvular prosthesis in a 38-year-old man treated for congenital aortic regurgitation. Horizontal long-axis gradient reversal MR image shows a huge signal void in the center of the heart (*V*). The signal void causes the size of the prosthesis to be exaggerated but otherwise does not prevent interpretation of the image.

aging. Valvular prostheses and arterial stents may produce artifacts that diminish diagnostic sensitivity (Fig 4), but examination in their presence is not precluded. Pregnancy is a relative contraindication. MR imaging may be performed if the benefit to the mother is deemed greater than the unknown risk to the fetus.



a.

b.

Figure 5. Use of a torso coil to increase signal. **(a)** Horizontal short-axis spin-echo MR image (two signals acquired) of a 68-year-old man with an infiltrating sarcoma (*S*) of the posterior wall of the left ventricle (*LV*) shows a clear difference in signal intensity between the epicardial fat and the free-wall myocardium of the right ventricle (arrowheads). The left main coronary artery is seen in cross section (arrow). Note the increased signal intensity of the anterior chest wall compared with that of the posterior chest wall. **(b)** Spin-echo MR image (same section as in **a**, four signals acquired) of a 50-year-old man evaluated for tricuspid regurgitation shows interventricular septal trabeculae in the right ventricle (arrows). However, the diagnostic quality of both images is nearly equal.

● Choosing Imaging Parameters

Regardless of the pulse sequence chosen, the number of signals acquired (NSA) will affect the spatial resolution of the image and the examination time. The greater the NSA, the greater the signal-to-noise ratio (SNR) of a voxel. The SNR of a voxel increases by the square root of the NSA used (eg, doubling the NSA from two to four increases the SNR by nearly 41%). On the other hand, increasing the NSA prolongs the examination time. Furthermore, prolonging the examination only increases patient restlessness, which often results in motion artifacts. We have found that using four signals acquired in our conventional spin-echo acquisition protocols provides superior imaging without unnecessarily prolonging examination time. Commercially available wraparound chest coils may be used to improve SNR. By placing the receiver closer to the body part being interrogated, sig-

nal is increased. We have found that such devices allow acquisition of spin-echo images with two signals acquired at no cost to image quality (Fig 5). Cine acquisitions performed with two signals acquired provide adequate spatial resolution and SNR in reasonable acquisition times.

Increasing section thickness increases the signal recovered but also results in loss of spatial resolution due to the greater amount of tissue interrogated. Generally, 8–10-mm-thick sections in adult patients and 5–8-mm-thick sections in children provide sharp images without significant loss of spatial resolution (increased spatial resolution is limited by the increasing noise found with thinner sections). Thinner sections may be acquired by imaging small children within a head coil or by using a torso coil with an adult.

The section-selection gradient is perpendicular to the phase- and frequency-encoding directions. Motion in the phase-encoding direction causes a banding artifact along the direction of the applied gradient. Suitable selection of the phase-encoding direction can minimize this artifact. During spin-echo acquisition, the phase-encoding gradient is switched on for a relatively short time in comparison with the frequency-encoding gradient. Motion occurring during phase encoding acquires only a small phase shift. Similar motion occurring during application of the frequency-encoding gradient acquires a greater phase shift, which creates greater artifact. Therefore, motion artifact can be minimized if the phase-encoding direction is horizontal during sagittal acquisition and vertical during coronal acquisition (9). In axial acquisition, most motion (blood flow) is through the imaging plane; there is little difference in image quality between horizontal or vertical phase encoding. In addition, the phase-encoding direction should be chosen to minimize the amount of tissue outside the field of view to avoid wraparound artifacts.

■ PERFORMING THE EXAMINATION

The MR imaging examination is limited to some extent by patient anxiety caused by confinement within a narrow magnet bore, coil noise, and study duration (10,11). In addition, adult patients with congenital or acquired heart disease are often mildly hypoxic and tend to be truly claustrophobic; thus, such patients often require sedation for MR imaging. If these patients are accompanied by a friend or relative who can transport them from the imaging facility, then they may be studied as outpatients. An occasional patient may not respond to mild, outpatient sedation. In this situation, as well as in patients with severe cyanosis or hemodynamic instability, MR imaging should be performed as an inpatient procedure with appropriate anesthesia backup as needed.

● Preparing for Imaging

Most patients who need mild sedation may be given 2-10 mg of diazepam by mouth; if the patient is unusually anxious, 2-20 mg of diazepam may be given intravenously and slowly (1 minute for every 5 mg administered). Oral diazepam may take a while to achieve a desired anxiolytic ef-

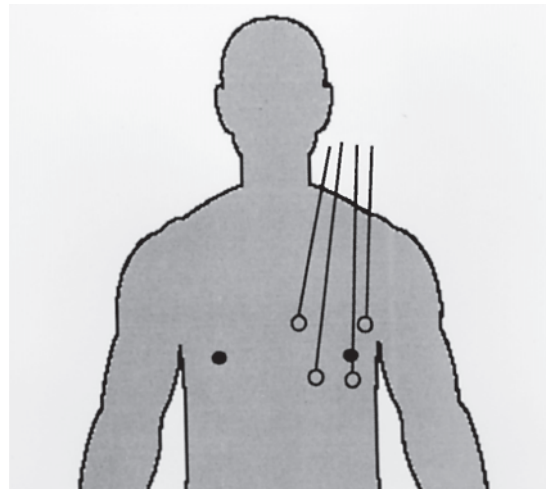


Figure 6. Placement of ECG leads. Leads should be placed within a 10-cm radius over the precordium. Wires should pass over the shoulder parallel to the long axis (B field) of the magnet.

fect, whereas intravenous administration has an immediate effect. The effect of light anesthesia in children is augmented if the child is deprived of sleep the night before the examination. Children may be sedated with orally or rectally administered chloral hydrate (up to 100 mg/kg) (12). Newborns may have their last feeding withheld and then be given a bottle of formula immediately before the examination. The newborn will fill its stomach and sleep without medication.

The ECG tracing obtained for gating cannot be used for diagnostic purposes. Peripheral pulse oximetry should be used in all sedated patients, any cyanotic patient, and any patient who has received intravenous contrast material. Hypoxic patients are especially sensitive to changes in ambient oxygen levels. Therefore, although it is unlikely that cryogenics used in superconducting magnet systems may vent into the examination room, the constant oxygen concentration of the examination room should be monitored.

An ideal team for performing cardiac MR imaging would include a radiologist experienced in managing cardiovascular disease, a nurse experienced in patient sedation and monitoring, and a technologist experienced in examining critically ill patients. MR facilities are often recent additions to an existing facility or in remodeled space, so resuscitation teams should be made aware of their location. Needless to say, complete "crash carts" should be readily available in all MR facilities.

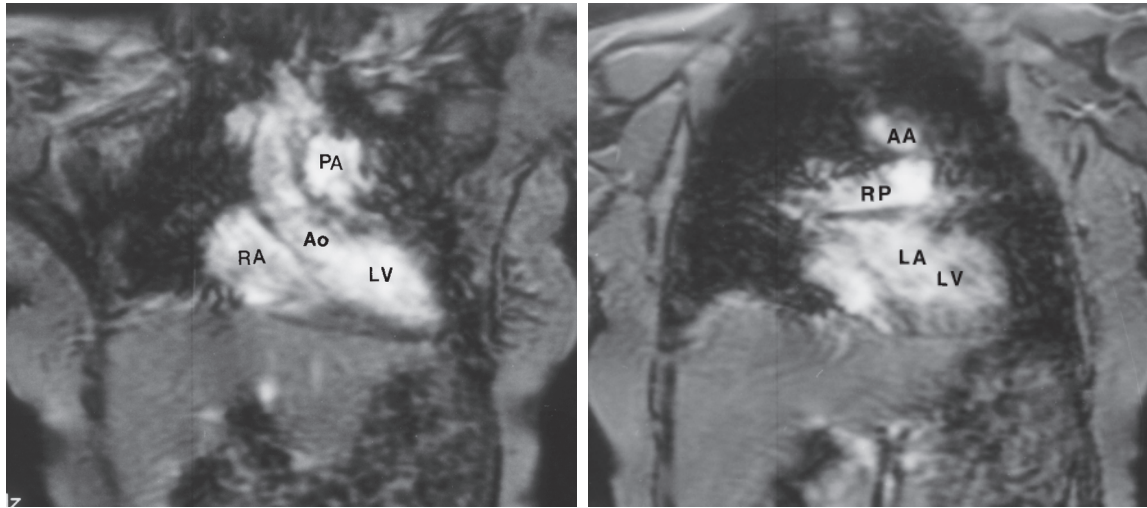


Figure 7. Scout images. **(a)** Coronal gradient reversal MR image (one signal acquired) shows the aortic root (*Ao*), left ventricle (*LV*), main pulmonary artery (*PA*), and right atrium (*RA*). **(b)** Coronal gradient reversal MR image (one signal acquired) obtained 3 cm posterior to **a** shows the distal aortic arch (*AA*), left atrium (*LA*), posterior left ventricle (*LV*), and right pulmonary artery (*RP*).

The ECG gating signal may be obtained by placing monitoring electrodes on the anterior or posterior chest wall (Fig 6); we prefer to apply leads to the anterior chest for patient comfort and ease of use. The ECGs of patients lying within an MR imager are degraded by superimposed electrical potentials resulting from the flow of blood in the magnetic field (13), the magnitudes of which are proportional to the magnetic field strength and are maximal when flow is perpendicular to the magnetic field lines. In a supine individual, the left ventricle and ascending aorta conduct blood nearly orthogonally to the magnetic field, a phenomenon that increases the amplitude of the T wave (14) and possibly confuses R-wave detection by the imager. Assignment of specific leads to each position is arbitrary; the combination of electrode placement and lead attachment that produces the tallest R waves with the least noisy background is the best lead selection. Superimposed blood flow-derived potentials may be minimized by application of electrodes relatively close together on the chest wall and by braiding the leads to avoid forming loops (15). The leads should not pass across the patient's chest and should be conducted out of the magnet bore parallel to the long axis of the magnet. We occasionally shave the patient's chest to ensure optimal contact with the ECG electrodes to provide a clear trac-

ing for ECG gating. However, as uncosmetic as such shaving may be, it is important to provide a clear ECG tracing for gating.

● Constructing Imaging Sections

The primary axes of the heart and left ventricle are not aligned parallel to the axes of the body. Evaluation in views orthogonal to body axes (axial, coronal, or sagittal) may distort the thickness of ventricular myocardium or the shape of the cardiac chambers. Specifically, in the supine position, the long axis of the body is parallel to the B field vector of the magnet but the long and short axes of the left ventricle are not. Thus, although image data obtained from axial, sagittal, or coronal acquisitions provide useful clinical information, these data may be degraded because the intracardiac anatomy is distorted by oblique acquisition. The size and shape of the ventricular cavity may be exaggerated and thus give a false impression of the functional state of the heart.

All cardiac MR imaging examinations in our department begin with a series of ungated gradient reversal "scout" images with one signal acquired in the coronal plane through the middle third of the chest (Fig 7). This rapid, low-resolution series provides cephalic and caudal landmarks for

the prescription of the next acquisition, a series of axial images. Most of our cardiac MR imaging examinations are spin-echo examinations supplemented by gradient reversal sequences performed to address specific functional questions.

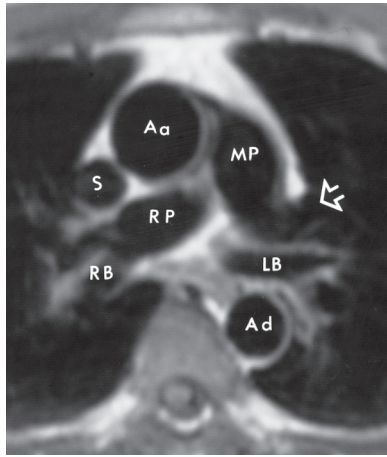
The advantage of acquiring axial cardiac images lies in the ease with which they are set up and the conventional manner in which anatomic data are presented. Axial chest MR images appear very similar to computed tomographic (CT) images obtained at the same anatomic level. Thus, individuals experienced in interpretation of chest CT images will immediately recognize details of intracardiac and mediastinal anatomy from axial MR images; the left-to-right and anterior-to-posterior relations among structures are apparent.

Axial images are necessary in the evaluation of any congenital heart lesion (Fig 8). The range of image acquisition with respect to the patient's long axis depends on the problem to be solved with MR imaging. In general, investigation of the aortic arch extends from cephalad to the aortic arch (to include the origins of the great

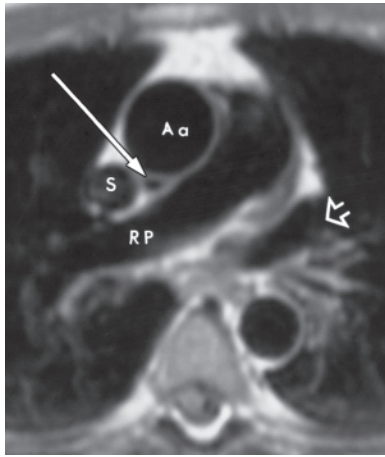
arteries) to just caudad to the aortic valve and left ventricular outflow tract. Examination of the heart and pericardium generally extends from just cephalic to the main pulmonary artery (the pericardial reflection) to just below the diaphragm. The latter landmark is chosen to demonstrate the intrahepatic inferior vena cava and the hepatic veins as well as the inferiormost portion of the pericardial space.

Examination of the left ventricle may be optimally performed with evaluation in the horizontal short-axis and four-chamber views, planes orthogonal to its intrinsic long and short axes. The football-shaped left ventricle has two orthogonal short axes, which form a plane orthogonal to the long axis of the ventricle. Construction of imaging planes orthogonal to intrinsic ventricular axes is based on identification of landmarks and starts with those identified in the initial scout series (Fig 7). Each successive acquisition provides the landmarks for the next acquisition and thus provides a logical and reproducible means of constructing rather complex, compound, angulated anatomic sections (Fig 9).

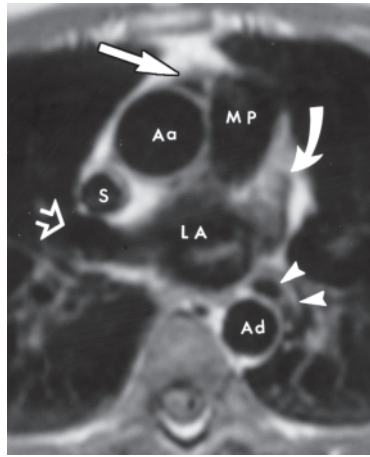
Figure 8. Series of axial spin-echo MR images with each image obtained 1 cm caudad to the previous one. **(a)** The ascending aorta (*Aa*), main pulmonary artery (*MP*), and superior vena cava (*S*) are outlined by mediastinal fat. The transverse portion of the right pulmonary artery (*RP*) is behind the aorta and superior vena cava and anterior to the right bronchus (*RB*). The left upper lobe pulmonary vein (arrow) is anterior to the left bronchus (*LB*). The descending aorta (*Aa*) lies to the left of the spine. **(b)** The left upper lobe pulmonary vein (open arrow) is seen entering the left atrium. Posterior to the ascending aorta (*Aa*), medial to the superior vena cava (*S*), and anterior to the right pulmonary artery (*RP*) is the signal void of the superior pericardial recess (solid arrow). **(c)** The signal void of the anterior aspect of the pericardial space (straight solid arrow) is seen between the ascending aorta (*Aa*) and proximal main pulmonary artery (*MP*). The right upper lobe pulmonary vein (open arrow) enters the left atrium (*LA*) posterior to the superior vena cava (*S*). The left lower lobe pulmonary vein (arrowheads) passes anterior to the descending aorta (*Aa*) before entering the left atrium. The left atrial appendage (curved arrow) forms the left border of the heart. **(d)** The left lower lobe pulmonary vein (*LI*) is seen entering the left atrium (*LA*). The three sinuses of the pulmonary artery may be identified (*1*, *2*, and *3*). **(e)** Just caudad to the pulmonary valve, the right ventricular outflow tract (*RVO*) is seen. The posterior left aortic sinus (*PLS*) is situated between the left atrium (*LA*) and right ventricular outflow tract. The trabeculated right atrial appendage (arrows) lies anterior to the root of the ascending aorta. **(f)** The entrance of the superior vena cava (*S*) into the right atrium and the ostium of the right atrial appendage (*RAA*) are seen. The commissures of the aortic valve define the anterior, posterior right, and posterior left aortic sinuses (*AS*, *PRS*, and *PLS*, respectively). The right lower lobe pulmonary vein (open arrow) enters the left atrium (*LA*). Note the fatty infiltration of the sinus venosus portion of the interatrial septum (solid arrows). **(g)** The signal void of the descending portion of the right coronary artery (arrow) is seen within the fat of the anterior atrioventricular ring. The posterior right aortic sinus (*PRS*) is interposed between the right atrium (*RA*) and left atrium (*LA*). The anterior mitral leaflet (arrowhead) is continuous with the aortic annulus. **(h)** The tricuspid valve (small white arrows) separates the right atrium (*RA*) from the right ventricle (*RV*). The muscular interventricular septum (black arrow) is shared by the right ventricle and left ventricle (*LV*). The atrioventricular septum (large white arrow) separates the left ventricle from the right atrium. The mitral valve separates the left atrium (*LA*) from the left ventricle. **(i)** The inferior vena cava (*IVC*) is seen entering the right atrium (*RA*). The coronary sinus (*C*) enters the right atrium medial to the increased-signal-intensity fat of the posterior atrioventricular ring (arrow).



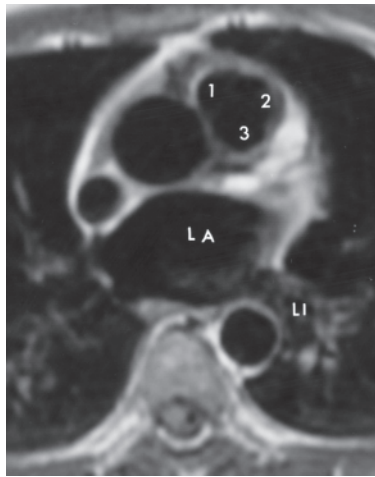
a.



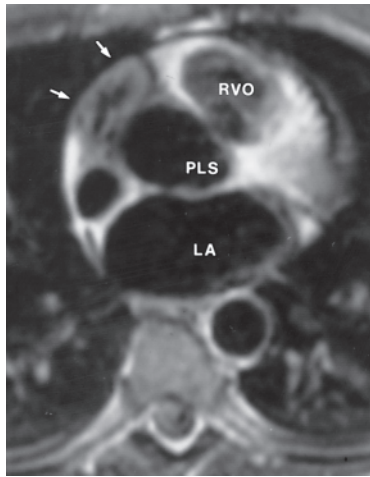
b.



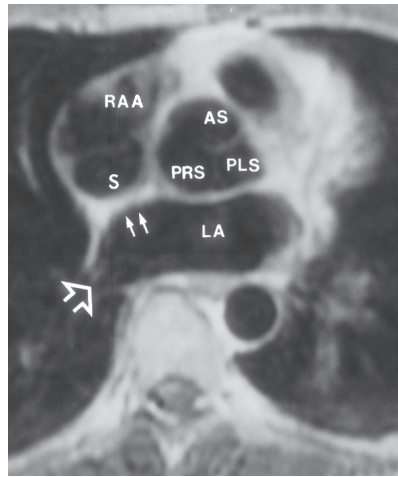
c.



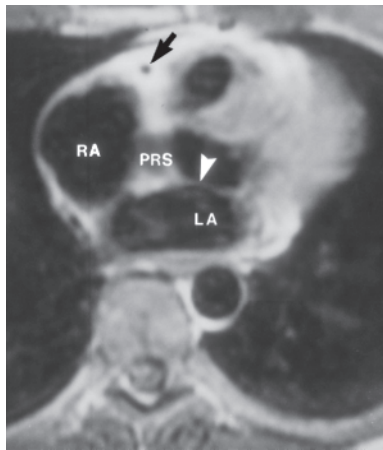
d.



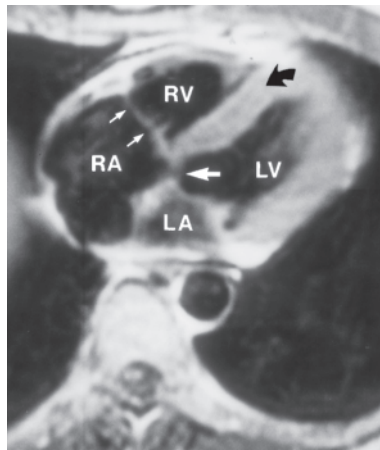
e.



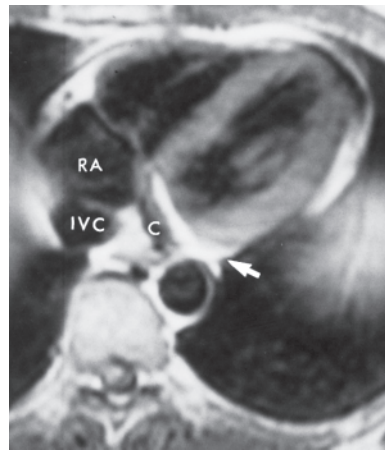
f.



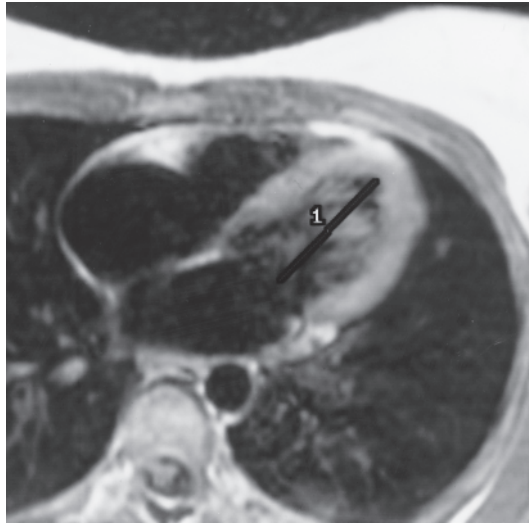
g.



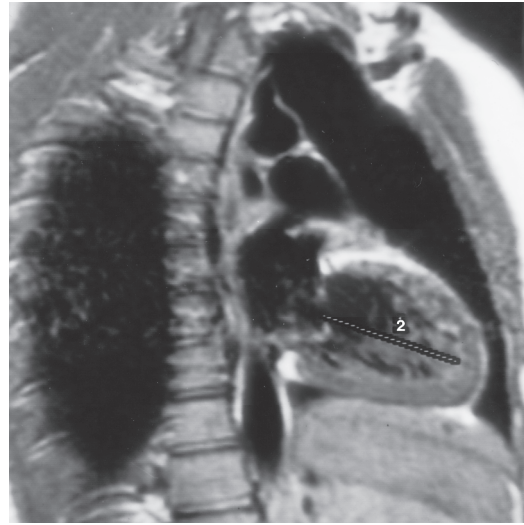
h.



i.

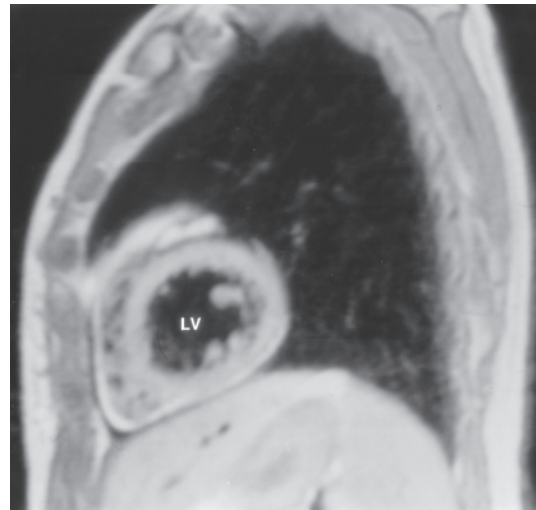


a.



b.

Figure 9. Constructing the left ventricular axes. **(a)** Axial spin-echo MR image shows a line (1) drawn between the middle of the mitral valve and the left ventricular apex. This line defines the plane containing the true long axis of the left ventricle. **(b)** Right anterior oblique sagittal MR image containing the mitral valve and left ventricular apex shows a line (2) drawn between the middle of the mitral valve and the left ventricular apex. This line defines the long axis of the left ventricle. Images obtained normal to this line are along the cardiac short axis. **(c)** Cardiac short-axis MR image shows the left ventricle (LV) as a round structure. The normal right ventricle seems to be an appendage of the left ventricle.



c.

From the coronal scout image through the middle of the heart, a section is obtained through the aortic valve and left ventricular apex. From this scout image, axial spin-echo images are obtained from the level of the pulmonary artery through the diaphragm. The image in this series that contains the left atrium, mitral valve, and left ventricular apex is chosen as the scout image for the next acquisition. A line drawn between the middle of the mitral valve and the apex of the left ventricle defines the plane containing the true long axis of the left ventricle. This plane is nearly parallel to the plane of the interventricular septum. Images obtained parallel to this plane are right anterior oblique sagittal images. From this series of right anterior oblique sagittal images, the image that best dem-

onstrates the mitral valve and cardiac apex is again chosen. In this image, a line drawn between the middle of the mitral valve and the left ventricular apex defines the long axis of the left ventricle. Images obtained orthogonal to this line are in the cardiac short-axis view.

When viewed in the short-axis section, the left ventricular myocardium appears as a series of intermediate-signal-intensity “doughnuts” surrounding the signal void (or increased signal intensity in gradient reversal acquisition) of the ventricular cavity. In diastole, the left ventricular myocardium in this section should be no more than 1 cm thick in normal adults and should be homogeneous in signal intensity. The left ventricular cavity appears as a circle in this view.

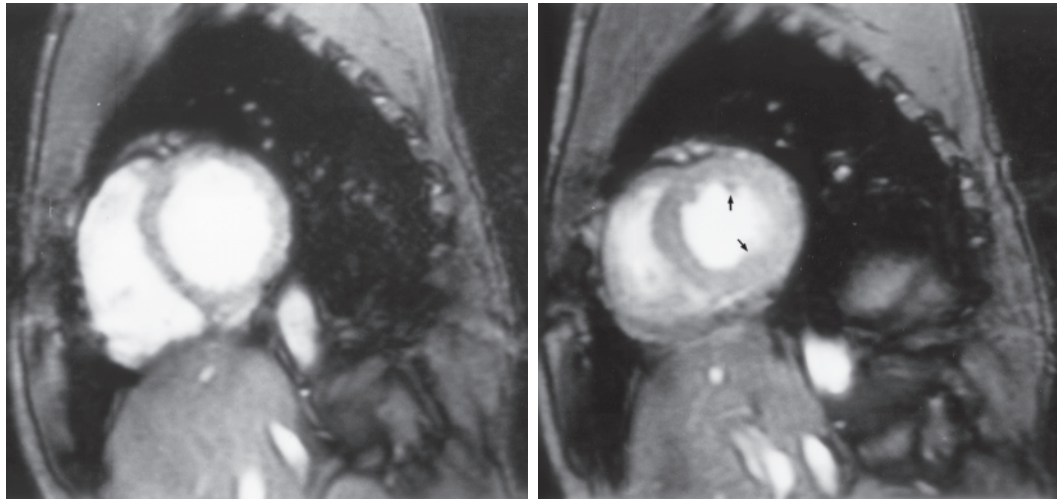


Figure 10. Short-axis section. **(a)** End-diastolic gradient reversal MR image shows a sharp border between the high-signal-intensity moving blood of the left ventricular cavity and the intermediate-signal-intensity myocardium. However, it is difficult to differentiate the right ventricular cavity from free-wall myocardium. **(b)** End-systolic gradient reversal MR image shows the papillary muscles of the posterior wall of the left ventricle more clearly (arrows). Left ventricular cavity size has decreased, and myocardial thickness has increased.

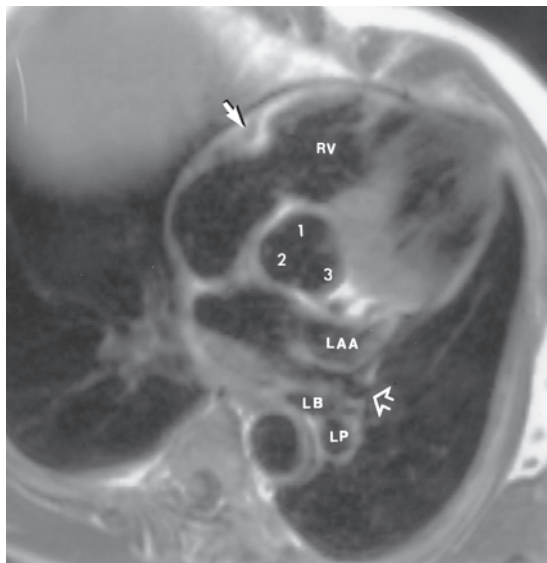
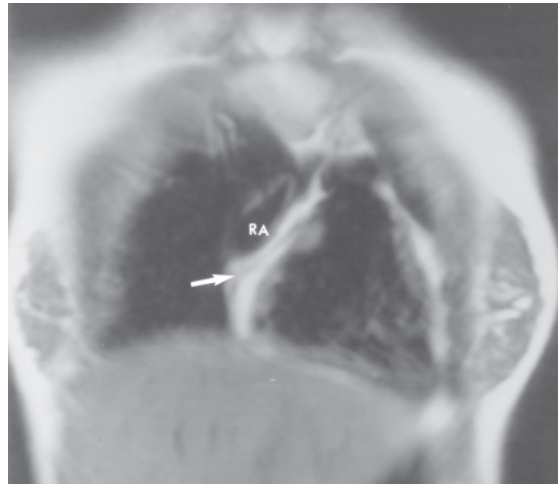
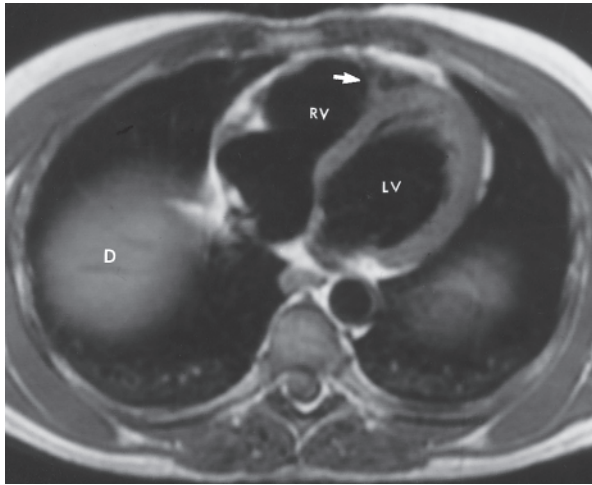


Figure 11. Four-chamber section. Spin-echo MR image shows the aortic sinuses (1, 2, and 3) in the center of the heart. Within the fat of the anterior atrioventricular ring lies the right coronary artery (solid arrow) and tricuspid valve. The trabeculated right ventricular (RV) free-wall myocardium is demonstrated. The anteroposterior relationships between the left atrial appendage (LAA) and left upper lobe pulmonary vein (open arrow) as well as the left bronchus (LB) and descending left pulmonary artery (LP) are well demonstrated.

The papillary muscles of the left ventricle appear as round loci of increased signal intensity (or signal voids in gradient reversal acquisition) in the lower left quadrant of the left ventricular cavity. Left ventricular cavity volume and myocardial mass may be accurately calculated with planimetry of the endocardial and epicardial ventricular borders viewed in this section (Fig 10).

The four-chamber view displays the heart in a series of parallel planes orthogonal to the short-axis sections (Fig 11). In this view, not only can the ventricular myocardium and ventricular chambers be evaluated but the aortic and mitral valves and their function may be scrutinized as well. The fibrous continuity between the two valve annuli is seen, and the alternation of mitral and aortic valvular opening and closing is demonstrated in cine mode. Regional changes in left ventricular myocardial thickness and cavity size are well displayed in this section.

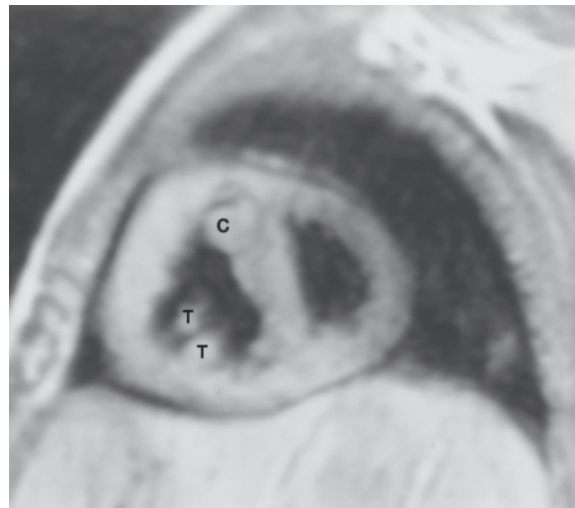
Evaluation of the right ventricle with orthogonal axial, sagittal, and coronal sections simplifies three-dimensional reconstruction of the unusual shape of the right ventricular cavity and



a.

b.

Figure 12. The right ventricle in orthogonal sections. (a) Axial spin-echo MR image at the level of the dome of the right diaphragm (*D*) shows the cavity of the right ventricle (*RV*) appearing to drape around the left ventricle (*LV*). The moderator band (arrow) is found on the right ventricular side of the interventricular septum and connects the free wall with the septum. (b) Coronal spin-echo MR image shows the cavity of the right ventricle extending from the fat of the anterior atrioventricular ring, which contains the signal void of the right coronary artery (arrow), to the fat of the anterior interventricular groove. The right atrial appendage (*RA*) is seen in cross section. (c) Sagittal spin-echo MR image of a patient with pulmonary hypertension and right ventricular hypertrophy clearly shows the hypertrophied right ventricular myocardial trabeculae (*T*) and supra-ventricular crest (*C*). Note the straightening of the interventricular septum.



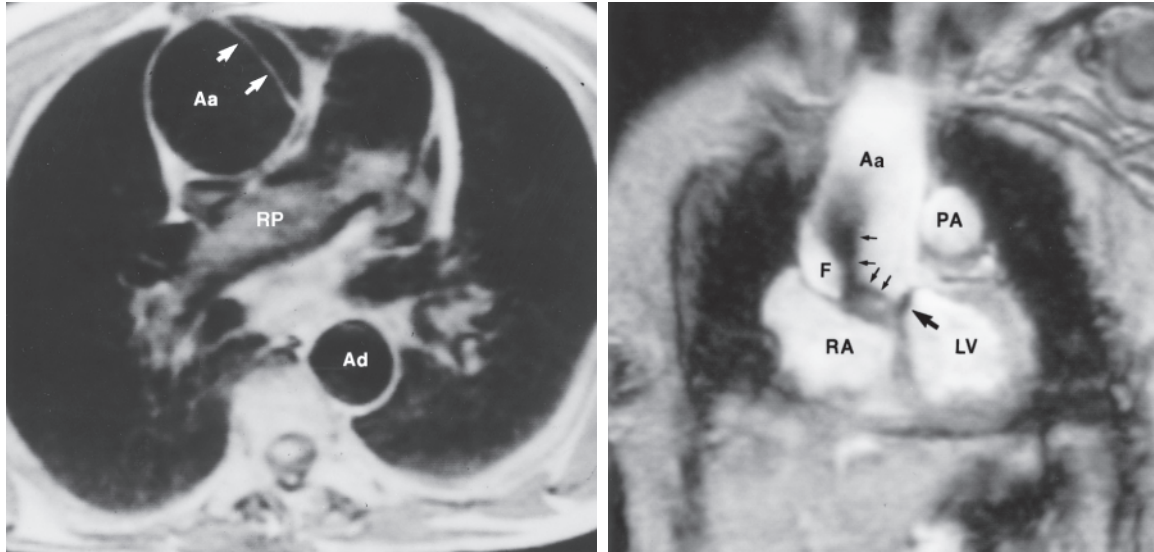
c.

provides landmarks for longitudinal and inpatient comparison of regional morphology (Fig 12). Quantitation of right ventricular myocardial thickening and ventricular function is reliably performed with oblique short-axis sections. Furthermore, since the left and right ventricles share the interventricular septum, quantitative (or even qualitative) analysis of short-axis images allows comparison of right with left ventricular function and evaluation of the role of the interventricular septum in cardiac function.

■ INDICATIONS FOR CARDIAC MR IMAGING

● Aortic Dissection

The most common diagnosis excluded with cardiac MR imaging is aortic dissection. The high contrast resolution, ability to image in arbitrary sections, and wide field of view for evaluating associated lesions make MR imaging a highly sensitive and extremely specific means of evaluating the thoracic aorta (16-18) (Fig 13). MR imaging is highly sensitive not only to the presence or absence of aortic dissection but for demonstration of the extent of the dissection, including entry and exit points, and extension



a. **b.**
Figure 13. Type I aortic dissection. **(a)** Axial spin-echo MR image through the transverse right pulmonary artery (*RP*) shows a dilated ascending aorta (*Aa*), which contains the high-signal-intensity intimal flap of the dissection (arrows). The descending aorta (*Ad*) is seen as a homogeneous signal void without a flap. **(b)** Off-coronal gradient reversal MR image through the aortic valve in another patient shows the dilated ascending aorta (*Aa*), left ventricle (*LV*), main pulmonary artery (*PA*), and right atrium (*RA*). A calcification of the aortic valve (large arrow) appears as a signal void in the aortic anulus. A jet of accelerating flow leaves the stenotic aortic valve and is deflected off the flap of an ascending aortic dissection into the true lumen of the mid-ascending aorta (small arrows). The false lumen (*F*) is separated from the true lumen.

of the dissection into one of the great arteries of the aortic arch as well as associated aortic insufficiency. This complete examination may be performed in a rapid, clinically relevant manner in clinically stable patients, as well as in many clinically unstable patients, by experienced examiners in an appropriately prepared setting.

Although hemodynamic stability is a precondition for MR imaging performed to exclude aortic dissection, one must assume the possibility of imminent cardiovascular collapse and act quickly to establish or exclude the diagnosis. From the coronal scout image, one prescribes dual spin-echo axial sections 10 mm thick with 1-mm intersection gaps. The repetition time is set according to the length of the patient's R-R interval. To maximize signal intensity, we usually prescribe a 20-msec echo time. When we acquire dual-echo images, we use echo times of 20 and 40 msec. The examination extends from

above the branches of the arch vessels to just below the aortic valve. If this territory cannot be covered in one acquisition, an additional acquisition in this plane is performed. An oblique sagittal spin-echo acquisition through the aortic arch (section thickness = 10 mm, intersection gap = 1 mm) displays the ascending aorta, aortic arch, and descending aorta in a plane orthogonal to the axial section and helps determine the extension of a dissection and possibly demonstrates entry and exit points. This acquisition is followed by an axial gradient reversal acquisition extending from the aortic valve and evenly spaced through the ascending aorta to demonstrate a thin, nonfatty intimal flap within a dilated aorta. The examination is completed with

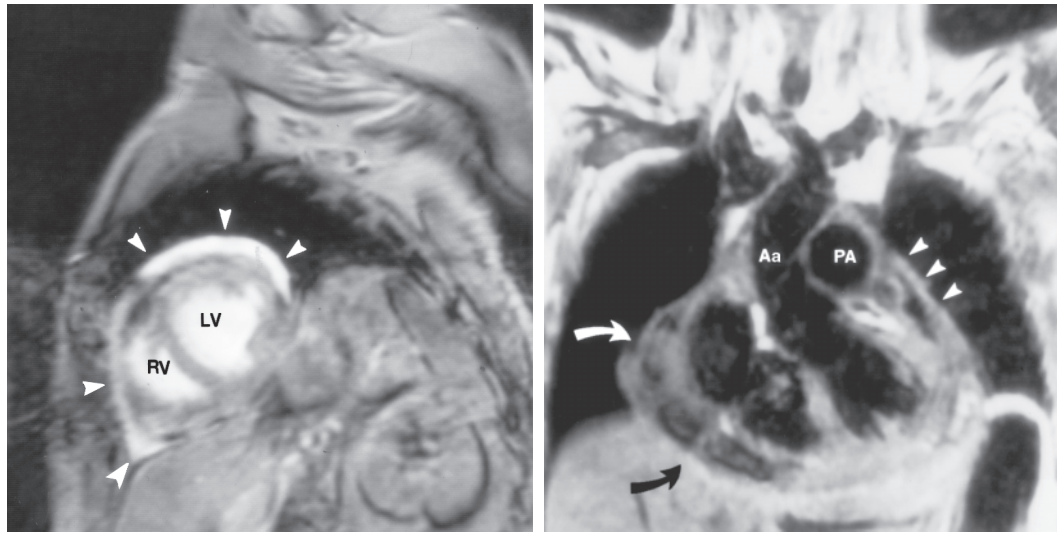


Figure 14. Pericardial disease. **(a)** Short-axis gradient reversal MR image obtained at end diastole in a 52-year-old man with congestive heart failure shows the right ventricular (*RV*) and left ventricular (*LV*) myocardium surrounded by a high-signal-intensity pericardial effusion (arrowheads). **(b)** Coronal spin-echo MR image of a 59-year-old woman with uremic pericarditis shows the attachment of the pericardium over the main pulmonary artery (*PA*) and ascending aorta (*Aa*). Note the thickened pericardium (arrowheads) as well as the increased-signal-intensity fibrinous exudate within the pericardial space (arrows).

a gradient reversal vertical long-axis acquisition through the aortic valve and left ventricular cavity to demonstrate the presence or absence of aortic regurgitation and the status of the left ventricular cavity and myocardial function. Spin-echo acquisitions are performed with two to four signals acquired (depending on the use of a chest coil); gradient reversal acquisitions are performed with two signals acquired.

● Evaluation of the Pericardium

ECG-gated cardiac MR imaging is an extremely important means of differentiating restrictive cardiomyopathy from constrictive pericarditis. In the latter, the pericardium may be thickened to at least 4 mm and thus increase the distance between the inner chamber of the heart and the outer cardiac borders (Fig 14). The ability to image in any arbitrary section allows MR imaging to demonstrate the entire pericardial space regardless of body habitus, thoracic deformity, or pulmonary hyperaeration. Furthermore, repeated images obtained over time may be compared for objective evaluation of the effects of medical or surgical therapy.

Complete examination of the pericardium (19–21) begins with a dual spin-echo acquisition extending from above the pulmonary ar-

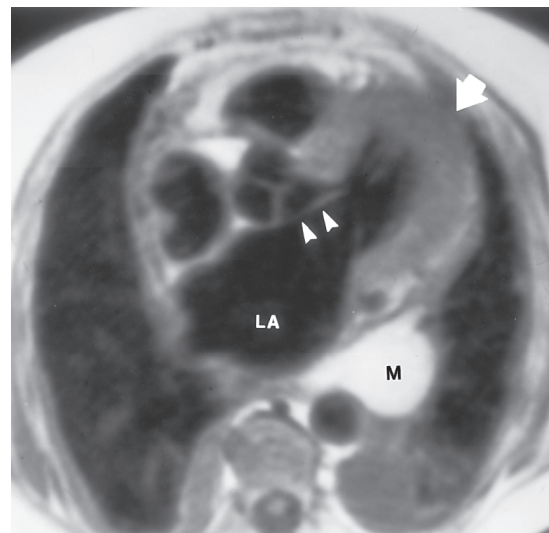
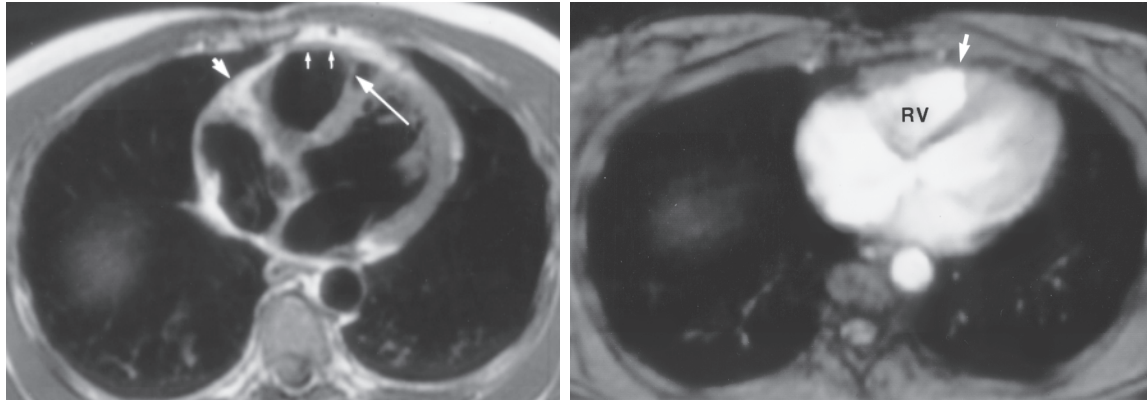


Figure 15. Ectopic fat in a 65-year-old man with shortness of breath. Axial spin-echo MR image shows a high-signal-intensity mass (*M*) immediately posterior to the left atrium (*LA*). The mass, which had been diagnosed as a mural left atrial tumor at echocardiography, is revealed to be mesenteric fat associated with a hiatal hernia. In addition, note the thickened left ventricular myocardium of hypertrophic obstructive cardiomyopathy (arrow) and especially the anteriorly displaced anterior mitral leaflet (arrowheads), which results in left ventricular outflow obstruction. Secondary signs of mitral regurgitation include left atrial enlargement and bilateral pleural effusions.



a. **b.**
Figure 16. Sustained ventricular tachycardia resulting from arrhythmogenic right ventricular dysplasia. **(a)** Axial spin-echo MR image of a 34-year-old man shows a thin veneer of epicardial fat that extends from the anterior atrioventricular ring (short large arrow) and then stops. The right ventricular free-wall myocardium (small arrows) from this point to the moderator band (long large arrow) is less than 2 mm thick. **(b)** Axial gradient reversal MR image of a 40-year-old woman with palpitations shows that a portion of the right ventricular (RV) free-wall myocardium fails to thicken (arrow). As a result, the right ventricular cavity appears to extend to the anterior chest wall.

tery (to include the pericardial reflection) to the upper abdomen (to include the hepatic veins and suprahepatic inferior vena cava). Acquisition of coronal or off-sagittal (right anterior oblique) sections should be added to demonstrate the infracardiac pericardial space and the lateral border of the right atrium. In patients with pericardial constriction, the dual spin-echo acquisition (vide supra) will provide sharp demonstration of the pericardium as well as the pericardial space and myocardial wall. Furthermore, analysis of signal intensities within the pericardial space will help differentiate masses from moving pericardial fluid.

Tumors of the heart and pericardium as well as paracardiac masses may be characterized according to their appearance and evaluated for possible medical or surgical therapy by using the multiplanar approach available with cardiac MR imaging. Demonstration of an intact pericardium or the presence of specific cardiac involvement provides useful information for accurate staging and for estimating clinical prognosis. Furthermore, differentiation of true paracardiac malignancy from ectopic or misplaced normal thoracic or abdominal contents (Fig 15) obviates expensive and potentially risky evaluation of such masses.

● Evaluation of Ventricular Function

Traditional evaluation of the left ventricle is based on modeling of its symmetric shape to that of a football. The right ventricle, on the

other hand, has no such axial or sagittal symmetry. Modeling of the right ventricle is difficult, and the variance between models and the actual appearance of the ventricle increases with the severity of right ventricular disease. Furthermore, MR imaging allows direct demonstration of fatty infiltration and failure of the right ventricular free-wall myocardium to thicken during systole, which are the basis for the radiologic diagnosis of arrhythmogenic right ventricular dysplasia (Fig 16).

Functional evaluation of the heart can be performed by assessing the morphology of the cardiac chambers and the myocardial wall thickness on serial images, but the value of cine acquisition cannot be overstated. Cine examination provides images of the cardiac chambers through the cardiac cycle and thus allows direct demonstration of temporal changes in cardiac morphology. Furthermore, cine acquisition demonstrates the cardiac chambers at end diastole and end systole and thus provides the substrate for calculation of ventricular myocardial mass (22,23) and chamber volume (24,25). Protocols for acquisition of quantitative information are predicated on short-axis gradient reversal acquisition. The first image in the series obtained at a particular section is the end-diastolic phase (be certain of the phase of the cardiac cycle if you are using peripheral pulse gating).

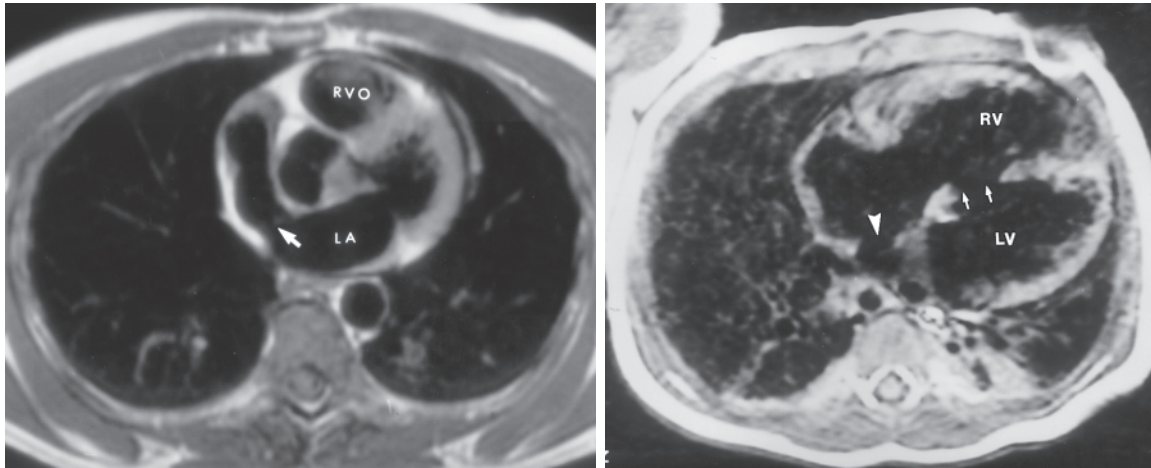


Figure 17. Intracardiac shunts. **(a)** Axial spin-echo MR image of a 26-year-old man with a sinus venosus atrial septal defect shows that the superior portion of the interatrial septum is incomplete (arrow). There is dilatation of the right ventricular outflow tract (*RVO*) and a normal-size left atrium (*LA*). **(b)** Axial spin-echo MR image of a 4-month-old boy with a large ventricular septal defect and a primum atrial septal defect shows a discontinuity in the interventricular septum (arrows) and a break in the posterior medial interatrial septum (arrowhead). Note the increased myocardial thickness and cavity size of the right ventricle (*RV*) and the dilatation of the left ventricle (*LV*).

The end-systolic phase is that image at a particular section with the minimum cavity area. Ventricular volume is computed as the sum of the cavity volume of each section (cavity area \times section thickness) over the entire chamber. Myocardial mass is calculated by summation of myocardial section mass ([epicardial area – cavity area] \times section thickness) over the entire ventricle (Table).

● Congenital Heart Disease

Examination of patients with congenital heart disease begins with axial images obtained from a coronal scout image. Acquisition should extend from the level of the aortic arch to below the diaphragm to include the inferior vena cava and hepatic veins. This larger imaging range facilitates demonstration of lesions associated with the specific clinical question as well as unsuspected additional lesions. Shunt lesions may be small and may not be directly demonstrated with spin-echo acquisition. However, if a shunt is present, one can expect to find sequelae of the shunt including chamber and arterial dilatation. Furthermore, covering the same anatomic territory with a gradient reversal sequence may help by directly demonstrating the jet of a shunt. Images in children should be thinner than in adults (5–8 mm). Since children have higher heart rates, their R-R intervals and thus calculated repetition times are shorter; each acquisi-

Right and Left Ventricular Volume and Myocardial Mass

Parameter by Ventricle	Value*
Right ventricle	
End-diastolic volume (mL/m ²)	67.9 \pm 13.4
End-systolic volume (mL/m ²)	27.9 \pm 7.5
Stroke volume (mL/m ²)	40.1 \pm 9.7
Ejection fraction	0.59 \pm 0.09
Mass (g/m ²)	23.3 \pm 1.4
Left ventricle	
End-diastolic volume (mL/m ²)	68.9 \pm 13.1
End-systolic volume (mL/m ²)	27.1 \pm 7.8
Stroke volume (mL/m ²)	41.8 \pm 10.9
Ejection fraction	0.60 \pm 0.11
Mass [†] (g/m ²)	91.6 \pm 3.2

Source.—References 22 and 24.

*Mean \pm standard deviation.

[†]The mass of the interventricular septum is assigned to the left ventricle.

tion therefore has fewer sections, but the higher heart rate reduces the duration of each acquisition. Careful examination with axial sections will reveal the defect itself or associated findings pointing toward one diagnosis or another (Fig 17). Orthogonal views provide additional findings that increase confidence in the diagnosis.

■ COMPLETING THE EXAMINATION

The MR imaging examination of a patient's heart is completed when the specific questions asked by the referring physician are satisfacto-

rily answered. Doing so requires the examining physician not only to be aware of the clinical indication for examination but also to be knowledgeable about associated issues related to particular clinical questions. For example, examination to exclude an intracavitary ventricular tumor is pretty straightforward; once the ventricular cavity has been completely displayed, the diagnosis is made or excluded and the examination can be terminated. On the other hand, evaluation of a patient with a dilated ascending aorta involves not only estimation of maximum aortic caliber (and the site of that dilatation) but evaluation of the aortic anulus, aortic valvular function, and the volume and mass of the left ventricle as well. Thus, increasing familiarity of examining physicians with the diseases being investigated will enhance their ability to use cardiac MR imaging to its fullest capacity.

■ REFERENCES

1. Boxt LM. MR imaging of congenital heart disease. *MR Clin North Am* 1996; 4:327-359.
2. Boxt LM. MR imaging of acquired heart disease. *MR Clin North Am* 1996; 4:253-268.
3. Lanzer P, Botvinick EH, Schiller NB, et al. Cardiac imaging using gated magnetic resonance. *Radiology* 1984; 150:121-127.
4. Lanzer P, Barta C, Botvinick EH, et al. ECG-synchronized cardiac MR imaging: method and evaluation. *Radiology* 1985; 155:681-686.
5. Lieberman JM, Alfid RJ, Nelson AD, et al. Gated magnetic resonance imaging of the normal and diseased heart. *Radiology* 1984; 152:465-470.
6. Pflugfelder PW, Sechtem U, White RD, Higgins CB. Quantification of regional myocardial function by rapid cine MR imaging. *AJR* 1988; 150:523-529.
7. Sechtem U, Pflugfelder PW, White RD, et al. Cine MR imaging: potential for the evaluation of cardiovascular function. *AJR* 1987; 148:239-246.
8. Hayes DL, Holmes DR Jr, Gray JE. Effect of 1.5 Tesla nuclear magnetic resonance imaging scanner on implanted permanent pacemakers. *J Am Coll Cardiol* 1987; 10:782-786.
9. Thickman D, Rubinstein R, Askenase A, Cabellero-Saez A. Effect of phase-encoding direction upon magnetic resonance image quality of the heart. *Magn Reson Med* 1988; 6:390-396.
10. Quirk ME, Letendre AJ, Ciottone RA, Lingley JF. Anxiety in patients undergoing MR imaging. *Radiology* 1989; 170:463-466.
11. Quirk ME, Letendre AJ, Ciottone RA, Lingley JF. Evaluation of three psychologic interventions to reduce anxiety during MR examination. *Radiology* 1989; 173:759-762.
12. Committee on Drugs, American Academy of Pediatrics. Guidelines for monitoring and management of pediatric patients during and after sedation for diagnostic and therapeutic procedures. *Pediatrics* 1992; 89:1110-1115.
13. Gaffey CT, Tenforde TS. Alterations in the rat electrocardiogram induced by stationary magnetic fields. *Bioelectromagnetics* 1981; 2:357-370.
14. Dimick RN, Hedlund LW, Herfkens RJ, et al. Optimizing electrocardiograph electrode placement for cardiac-gated magnetic resonance imaging. *Invest Radiol* 1987; 22:17-22.
15. Wendt RE III, Rokey R, Vick GW III, Johnston DL. Electrocardiographic gating and monitoring in NMR imaging. *Magn Reson Imaging* 1988; 6:89-95.
16. Nienaber CA, Spielmann RP, von Kodolitsch Y, et al. Diagnosis of thoracic aortic dissection: magnetic resonance imaging versus transesophageal echocardiography. *Circulation* 1992; 85:434-447.
17. Nienaber CA, von Kodolitsch Y, Brockhoff CJ, et al. Comparison of conventional and transesophageal echocardiography with magnetic resonance imaging for anatomical mapping of thoracic aortic dissection: a dual noninvasive imaging study with anatomical and/or angiographic validation. *Int J Card Imaging* 1994; 10:1-14.
18. Nienaber CA, von Kodolitsch Y, Nicholas V, et al. The diagnosis of thoracic aortic dissection by noninvasive imaging procedures. *N Engl J Med* 1993; 328:1-9.
19. Amparo EG, Higgins CB, Farmer D, et al. Gated MRI of cardiac and paracardiac masses: initial experience. *AJR* 1984; 143:1151-1156.
20. Masui T, Finck S, Higgins CB. Constrictive pericarditis and restrictive cardiomyopathy: evaluation with MR imaging. *Radiology* 1992; 182:369-373.
21. Mulvagh SL, Rokey R, Vick GW III, Johnston DL. Usefulness of nuclear magnetic resonance imaging for evaluation of pericardial effusions, and comparison with two-dimensional echocardiography. *Am J Cardiol* 1989; 64:1002-1009.
22. Katz J, Whang J, Boxt LM, Barst RJ. Estimation of right ventricular mass in normal subjects and in patients with primary pulmonary hypertension by nuclear magnetic resonance imaging. *J Am Coll Cardiol* 1993; 21:1475-1481.
23. Keller AM, Peshock RM, Malloy CR, et al. In vivo measurement of myocardial mass using nuclear magnetic resonance imaging. *J Am Coll Cardiol* 1986; 8:113-117.
24. Boxt LM, Katz J, Kolb T, et al. Direct quantitation of right and left ventricular volumes with nuclear magnetic resonance imaging in patients with primary pulmonary hypertension. *J Am Coll Cardiol* 1992; 19:1508-1515.
25. Sechtem U, Pflugfelder PW, Gould RG, et al. Measurement of right and left ventricular volumes in healthy individuals with cine MR imaging. *Radiology* 1987; 163:697-702.